

YerPhI Preprint-1624

N. M. Agababyan ¹⁾, L. Grigorian²⁾, N. Grigoryan²⁾, H. Gulkanyan ²⁾,
A. A. Ivanilov ³⁾, Zh. Karamyan ²⁾, V. A. Korotkov³⁾

**NUCLEAR ATTENUATION OF THREE-HADRON SYSTEMS
IN NEUTRINO-INDUCED REACTIONS**

¹⁾ Joint Institute for Nuclear Research, Dubna, Russia.

²⁾ Alikhanian National Scientific Laboratory, Yerevan, Armenia.

³⁾ Institute of High Energy Physics, Protvino, Russia.

Yerevan 2011

Abstract

For the first time, the nuclear attenuation of three hadron systems is studied in neutrino-induced reactions using the data obtained with SKAT bubble chamber. The strongest attenuation ($R_3 \sim 0.6$) is observed for a system carrying an overwhelming fraction of the current quark energy, as well as for a system with the smallest effective mass. An indication is obtained that the correlation effects in the nuclear attenuation play only a minor role. The experimental data are compared with predictions of the quark string fragmentation model.

1. INTRODUCTION

The investigation of the multihadron leptonproduction on nuclear targets can provide a valuable information on the space-time structure of the quark string fragmentation and the hadron formation ([1–4] and references therein). At present the experimental data on the double hadron production are available in electronuclear [5] and neutrino nuclear [6] interactions. This work is devoted to the study, for the first time, of the nuclear effects in the neutrino production of more complex, three hadron systems. In Section 2 the experimental procedure is described. The experimental data are presented and compared with theoretical predictions in Section 3. The results are summarized in Section 4.

2. EXPERIMENTAL PROCEDURE

The experiment was performed with SKAT bubble [7] chamber exposed to a wideband neutrino beam obtained with a 70 GeV primary protons from the Serpukhov accelerator. The chamber was filled with a propane-freon mixture containing 87 vol% propane (C_3H_8) and 13 vol% freon (CF_3Br) with the percentage of nuclei $\text{H}:\text{C}:\text{F}:\text{Br} = 67.9:26.8:4.0:1.3\%$. A 20 kG uniform magnetic field was provided within the operating chamber volume.

Charged current interactions containing a negative muon with momentum $p_\mu > 0.5 \text{ GeV}/c$ were selected. Other negatively charged particles were considered to be π^- mesons. Protons with momentum below $0.6 \text{ GeV}/c$ and a fraction of protons with momentum $0.6\text{--}0.85 \text{ GeV}/c$ were identified by their stopping in the chamber. To non-identified positively charged particles the pion mass was assigned. Events with errors in measuring the momenta of all charged secondaries and photons less than 60% and 100%, respectively, were selected. Each event was given a weight to correct for the fraction of events excluded due to improperly reconstruction. More details concerning the experimental procedure, in particular, the estimation of the neutrino energy

E_ν and the reconstruction of $\pi^0 \rightarrow 2\gamma$ decays, can be found in our previous publications [8,9,10]. In this work, $\gamma\gamma$ combinations with the effective mass $m_{\gamma\gamma}$ closest to $135 \text{ MeV}/c^2$ (and enclosed in the range of $105 < m_{\gamma\gamma} < 165 \text{ MeV}/c^2$) were taken, requiring the each detected γ to be included in no more than one $\gamma\gamma$ combination.

The events with $3 < E_\nu < 30 \text{ GeV}$ were accepted provided that the reconstructed mass W of the hadronic system exceeds 2 GeV and $y = \nu/E_\nu < 0.95$, ν being the energy transferred to the hadronic system. No restriction was imposed on the transfer momentum squared Q^2 . The number of accepted events was 4499 (5683 weighted events). The contamination from the neutral current (NC) interactions to the selected event sample was estimated to be $(2.6 \pm 0.2)\%$. The mean values of the kinematic variables were $\langle E_\nu \rangle = 10.0 \text{ GeV}$, $\langle W \rangle = 2.9 \text{ GeV}$, $\langle W^2 \rangle = 9.1 \text{ GeV}^2$, $\langle Q^2 \rangle = 2.7 (\text{GeV}/c)^2$ and $\langle \nu \rangle = 5.8 \text{ GeV}$.

The nuclear attenuation effects studied below are inferred with the help of a comparison of the trihadron characteristics in two event subsamples: the nuclear subsample (B_A) and quasinucleon subsample (B_N) composed using a number of topological and kinematical criteria [8, 9]. The B_N subsample includes events with no indication of the nuclear disintegration or a secondary intranuclear interaction: the total charge of secondary hadrons is required to be $q = +1$ (for the subsample B_n of interactions with a neutron) or $q = +2$ (for the subsample B_p of interactions with a proton), while the number of recorded baryons (these included identified protons and Λ -hyperons, along with neutrons that suffered a secondary interaction in the chamber) was forbidden to exceed unity, baryons flying in the backward hemisphere being required to be absent among them. Moreover, a constraint was imposed on the effective target mass $M_t < 1.2 \text{ GeV}/c^2$, the M_t being defined as $M_t = \Sigma(E_i - p_i^L)$ where the summation is performed over the energies E_i and the longitudinal momenta p_i^L (along the neutrino direction) of all recorded secondary particles. Events that did not satisfy aforementioned criteria were

included in the subsample B_S of cascade events. As a result, the weighted numbers of the B_p , B_n and B_S proved to be 1249, 1304 and 3129.

The validity of the selection of the B_p and B_n subsamples was verified [9, 11, 12] by comparison of a large number of the multiplicity and spectral characteristics of hadrons in these subsamples with the available data obtained on hydrogen and deuterium targets, resulting in a satisfactory agreement and giving a sufficient ground to conclude that the B_p and B_n subsamples may contain only a minor contamination from events where the secondary intranuclear interactions deteriorate the characteristics of the primary hadrons. We checked the sensitivity of the extracted data (presented in the next section) relative to the choice of the boundary value of M_t , varying the latter from 1.1 to 1.4 GeV/ c^2 , e.g. changing the event numbers in the B_p , B_n and B_S subsamples and continuously increasing the contamination from secondary interactions in the subsamples B_p and B_n (see Fig. 1 in [11]). We found that the variation of the dihadron characteristics have been on an average fivefold smaller as compared to the statistical errors.

As it follows from the composition of the propane-freon mixture (see above) about 36% of sub-sample B_p is contributed by interactions with free hydrogen (at the ratio of νn and νp CC cross sections being equal to 2). Weighting the quasiproton events with a factor of 0.64, one can compose a pure nuclear subsample $B_A = B_S + B_n + 0.64B_p$ and a quasinucleon subsample $B_N = B_n + 0.64B_p$. As it follows from the percentage of C, F and Br nuclei in the propan-freon mixture the mean atomic weight of the composite target is equal to $\overline{A} = 27.6$ for neutrino-nuclear interactions. However, since the nuclear attenuation effects are under consideration, it seems more relevant to introduce an effective nucleus A_{eff} in which the probability of the hadron absorption is the same as that obtained from averaging over the target nuclei. The calculations (see [13] for details) result in $19 \leq A_{\text{eff}} \leq 23$, depending on the momentum of the neutrino-produced hadron.

3. THE RESULTS

Below we will consider hadrons produced in the forward hemisphere in the hadronic c.m.s. (i.e. in the region of $x_F > 0$, x_F being the Feynman variable), because in this region the nuclear attenuation effects for hadrons dominate over multiplication effects caused by secondary intranuclear inelastic interactions, observable in the region of $x_F < 0$ and, to a much smaller extent, even in the region of $0 < x_F < 0.1$ [9,11]. Below we will imply two different cuts on x_F : $x_F > 0$ and $x_F > 0.1$.

For a given kinematic variable v , characterizing a trihadron, the nuclear attenuation is measured by the ratio $R_3(v) = n_3^A(v)/n_3^N(v)$, where $n_3^A(v)$ and $n_3^N(v)$ are the trihadron differential mean multiplicities (yields) in the nuclear and quasinucleon subsamples, respectively.

Figure 1 (top panel) shows the dependence of R_3 on the maximal angle ϑ^{\max} between two hadrons entering into the three-hadron system. The data exhibit a strengthening attenuation with decreasing ϑ^{\max} which can be caused by secondary intranuclear interactions, mainly elastic for the case of $x_F > 0.1$ and both elastic and inelastic for the case of $x_F > 0$. The elastic scattering of hadrons also leads to the increasing effective mass m_{eff} of the trihadron and hence to a stronger attenuation at smaller m_{eff} than at larger m_{eff} , as it is seen from the middle panel of Figure 1 for $x_F > 0.1$. On the other hand, the inelastic interactions (playing more significant role at the cut $x_F > 0$) lead to energy losses of hadrons which partly compensate the effective mass increasing caused by the widening of the angles between scattered hadrons, as it can be concluded from the middle panel of Figure 1 where a rather flat m_{eff} - dependence is observed for the case of $x_F > 0$.

The bottom panel of Figure 1 shows the dependence of the ratio $R_3(p_t)$ on the trihadron transverse momentum p_t (defined relative to the current quark direction). A trend of increasing $R_3(p_t)$ with increasing p_t is observed, being a consequence of secondary interactions of neutrino-produced hadrons.

It should be noted, that a characteristic feature of the data presented in Figure 1 is that, in general, the ratio $R_3(v)$ at $x_F > 0$ exceeds that for the case of $x_F > 0.1$, indicating, as it was already mentioned above, that a non-negligible fraction of low x_F hadrons (with $0 < x_F < 0.1$) originates from inelastic intranuclear interactions of higher - x_F hadrons.

Figure 2 presents the dependence of the ratio R_3 on the collective variable $Z = \sum z_k$, where $z_k = E_k/\nu$ with E_k being the energy of the k -th hadron and the sum is over three hadrons. For comparison, we also plotted the ratio $R_2(z)$ versus $Z = z_1 + z_2$ for two-hadron systems and the ratio $R_1(z)$ versus the z value for single hadrons. As it is seen, both functions R_1 , R_2 and R_3 continuously decrease with the increasing argument. It worths to note, that the fastest single hadron (with $z > 0.85$) absorbs stronger than the fastest hadron systems (with the same summary Z) composed of two or three hadrons of smaller z 's.

It is also interesting to compare the ratio $R_1(z)$ for single hadron with the ratios $R_2(z)$ and $R_3(z)$ where the argument refers to a hadron (the "trigger" hadron) accompanied by, respectively, one and two hadrons of arbitrary values of the variable z . A decreasing n -dependence of $R_n(z)$, seen in Figure 3 and, more clearly, in Figure 4 and 5, is related to the additional attenuation of the accompanying hadron(s). The n -dependencies of $R_n(z)$ plotted in Figure 4 (at $x_F > 0$) and 5 (at $x_F > 0.1$) can be approximated as $R_n(z) = \rho_1(z)(1 - w_1)^{n-1}$, where $\rho_1(z)$ is the attenuation ratio for the 'trigger' hadron, while w_1 is the mean absorption probability of a single hadron averaged over hadrons accompanying the 'trigger' one. As it is seen from the fitted values of $\rho_1(z)$ and w_1 quoted in Figures 4 and 5, the ratio $\rho_1(z)$ is maximal for the slowest trigger hadron (even exceeding unity at $x_F > 0$ due to the nuclear enhancement effects). At higher z -values, the variation of $\rho_1(z)$ is not significant, while the values of w_1 are around $w_1 \sim 0.05$ at $x_F > 0$ and around $w_1 \sim 0.12$ at $x_F > 0.1$. These w_1 values are averaged over a wide range of the z variable of accompanying hadrons. A more definite

estimation for the absorption probability can be inferred from the n -dependence of $R_n(z)$ at a narrow z -range of all involved hadrons, for example, at $0.1 < z < 0.33$ (see Figure 6). Under assumption that hadrons absorb independently with a mean probability w_{abs} , the n -dependence of $R_n(z)$ can be expressed as $R_n(z) = (1 - w_{\text{abs}})^n$. The data at $x_F > 0$ are described by this dependence quite well (with the fit value $w_{\text{abs}} = 0.060 \pm 0.006$), being consistent with the assumption that the correlated absorption effects do not play a prominent role (Figure 6, the left panel). The description of the data at $x_F > 0.1$ (with the fit value $w_{\text{abs}} = 0.077 \pm 0.014$) is somewhat worse, due to a possible (statistically not provided) deviation of the R_3 value from the general trend of the n -dependence of R_n . It can be a faint manifestation of the mutual screening effect (suggested in [4]) in the system of hadrons produced at close impact parameters. Statistically more provided data are needed to check this assumption.

It should be also noted, that the observed difference between w_1 and w_{abs} (quoted in Figures 5 and 6 for the case of $x_F > 0.1$) can be caused by the fact that the latter concerns the hadrons with $0.1 < z < 0.33$ at which the hadron formation length is expected to be maximal (hence reducing their absorption), while the former concerns the hadrons which can carry larger z 's at which the formation length is comparatively shorter [14].

We undertook an attempt to describe our data in the framework of the Two-Scale Model (TSM) [15] (see also [4] and references therein) which was already applied for description of our data on the nuclear attenuation of neutrino-produced two-hadron systems [6]. The details of the TSM application to three-hadron systems can be found in [16]. The TSM contains four free parameters: the quark string tension κ and the following string-nucleon interaction cross sections, namely, σ_q for the initial string stretched between the struck quark and the target nucleon remnant, σ_s for the intermediate string stretched between the struck quark and a created antiquark (which becomes a valence one for the hadron being looked at) and σ_h for the formed colorless

system with quantum number and valence content of the final hadron.

As it was shown in [6], a reasonable agreement with the data on the two-hadron neutrino production can be reached at the following set of the model parameters: $\kappa = 0.8$ GeV/fm. $\sigma_q = 0$, $\sigma_s = 10$ mb and $\sigma_h = 20$ mb. This set was used to get the TSM predictions presented below. The predictions concern pions, pion pairs and pion triplets. In present calculations, only the z variable of produced pions is considered, while the x_F variable does not appear explicitly in the model. Therefore, the same predictions of the model are compared below, in Figs. 2, 3, 4, 5 and 6, with experimental data inferred both at $x_F > 0$ and $x_F > 0.1$.

As it is seen, the description of the data at $x_F > 0$ is noticeably worse, probably, due to the aforementioned effects of intranuclear interactions (not inserted into the model) leading to a significant enhancement of the yield of low- z hadrons (especially in the region of $z < 0.2$) and, as a consequence, the yields of dihadrons and trihadrons with comparatively small values of $Z < 0.3 \div 0.4$. At a more severe restriction on $x_F > 0.1$, the said discrepancy is much smaller, and the model provides a reasonable description of the data at $Z > 0.2$, as it can be seen from Figs. 2 and 3. An exception is $R_1(z)$ for the fastest single hadron with $z > 0.85$ for which the model badly underestimates the nuclear attenuation. On the other hand, the model predictions are compatible with the data at the the same summary Z -range ($Z \sim 0.9$) for hadron systems composed of two or three hadrons with smaller individual z 's (see Fig. 2). The TSM describes quite well the n -dependence of the ratio $R_n(z)$ at z -values of the trigger hadron above $z = 0.22$, as it can be seen from Fig. 3 (the right panel) and Fig. 5 (the middle and right panels). It should be also noted, that the TSM predictions for the slope in the n -dependence of $R(z)$ (the dashed lines in Fig. 5) at $z > 0.22$ are rather close to those extracted under assumption of an independent absorption of neutrino-produced hadrons (the solid lines in Fig. 5). The same can be said about the slopes in the n -dependence of R_n for the case when all involved

hadrons are enclosed in a narrow z -range of $0.1 < z < 0.33$, as it is seen from Fig. 6 where the model predictions are plotted by dashed lines. The predicted values of R_n , however, underestimate the experimental data, probably, due to the unsufficiently large values of the variable z (see the discussion above).

4. SUMMARY

The nuclear attenuation of three-charged hadron systems is studied for the first time in neutrino-induced reactions.

The dependence of the attenuation factor R_3 on various kinematic variables of the trihadron is investigated. The strongest attenuation, with $R_3 \sim 0.6$, is observed for a system of hadrons with $x_F > 0.1$ having the smallest effective mass, as well as at largest values of the collective variable Z . The observed dependence of R_n on the number n of involved hadrons enclosed in the narrow range of $0.1 < z < 0.33$ is compatible with an assumption that the intranuclear interaction of a hadron occurs with a mean probability $w_{\text{abs}} = 0.07 \pm 0.02$ and almost independently of accompanying hadrons.

It is shown, that the Two-Scale Model of the quark string fragmentation provides a reasonable description of the nuclear attenuation for systems composed of relatively energetic ($x_F > 0.1$ and $z > 0.2$) hadrons.

ACKNOWLEDGMENTS

The authors from YerPhI acknowledge the supporting grants of Calouste Gulbenkian Foundation and Swiss Fonds Kidagan. The activity of two of the authors (L.G. and H.G.) is supported by Cooperation Agreement between DESY and YerPhI signed on December 6, 2002.

References

- [1] A.Bialas and J.Czyżewski, Z. Phys. C **47**, 133 (1990)
- [2] J.Czyżewski, Phys. Rev. C **43**, 2426 (1991)
- [3] A.Majumder, Eur. Phys. J. C **43**, 259 (2005)
- [4] N.Akopov, L.Grigoryan, Z.Akopov, Eur. Phys. J. C **44**, 219 (2005); *ibid.* C **49**, 1015 (2007)
- [5] A.Airapetian *et al.*, Phys. Rev. Lett. **96**, 162301 (2006)
- [6] N.M.Agababyan *et al.*, Phys. Atom. Nucl. **74**, 246 (2011)
- [7] V.V.Ammosov *et al.*, Fiz. Elem. Chastits At. Yadra **23**, 648 (1992)
- [8] N.M.Agababyan *et al.*, Preprint No.1535, YerPhI (Yerevan, 1999)
- [9] N.M.Agababyan *et al.*, Yad. Fiz. **66**, 1350 (2003)
- [10] N.M.Agababyan *et al.*, Phys. Atom. Nucl. **74**, 221 (2011)
- [11] N.M.Agababyan *et al.*, Preprint No.1578, YerPhI (Yerevan, 2002)
- [12] N.M.Agababyan *et al.*, Yad. Fiz. **68**, 1209 (2005)
- [13] N.M.Agababyan *et al.*, Yad. Fiz. **70**, 1777 (2007)
- [14] A.Bialas, M.Gyulassy, Nucl. Phys. B **291**, 793 (1987)
- [15] J.Ashman *et al.*, Z. Phys. C **52**, 1 (1991)
- [16] L.Grigoryan, arXiv: 1103.4519 [hep-ph] 2011

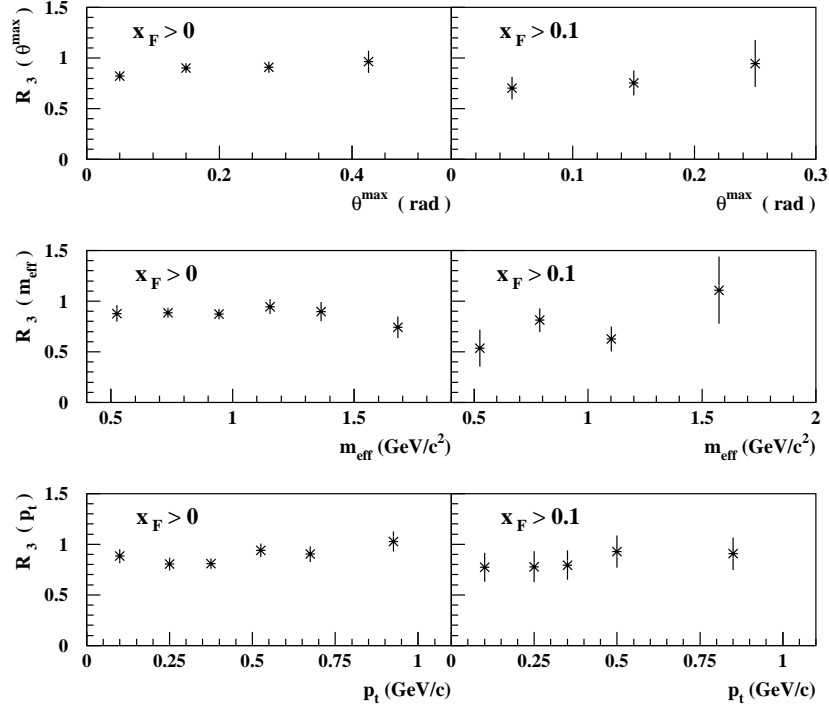


Figure 1: The dependence of R_3 on v^{\max} (top panels), m_{eff} (middle panels) and p_t (bottom panels) for hadrons with $x_F > 0$ (left panels) and $x_F > 0.1$ (right panels).

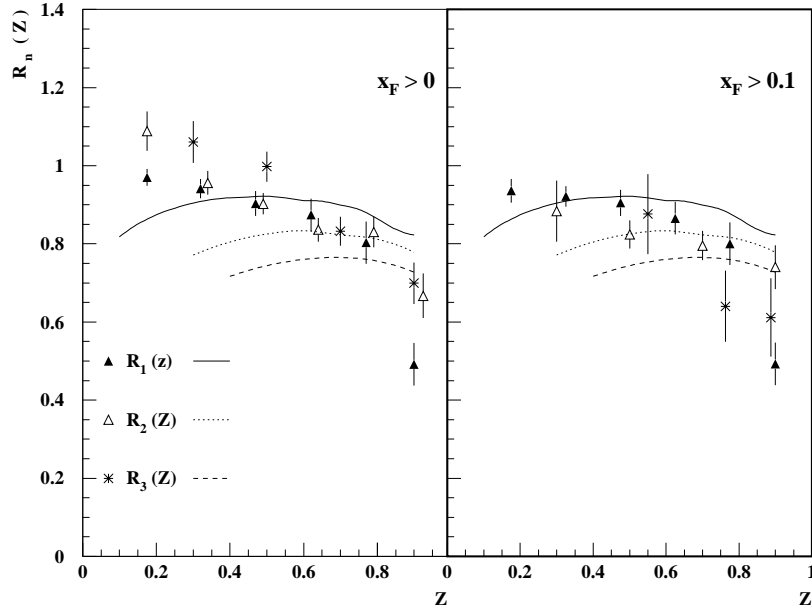


Figure 2: The dependence of R_n ($n = 1, 2, 3$) on Z for hadrons with $x_F > 0$ (left panel) and $x_F > 0.1$ (right panel) The curves are the TSM predictions (see text).

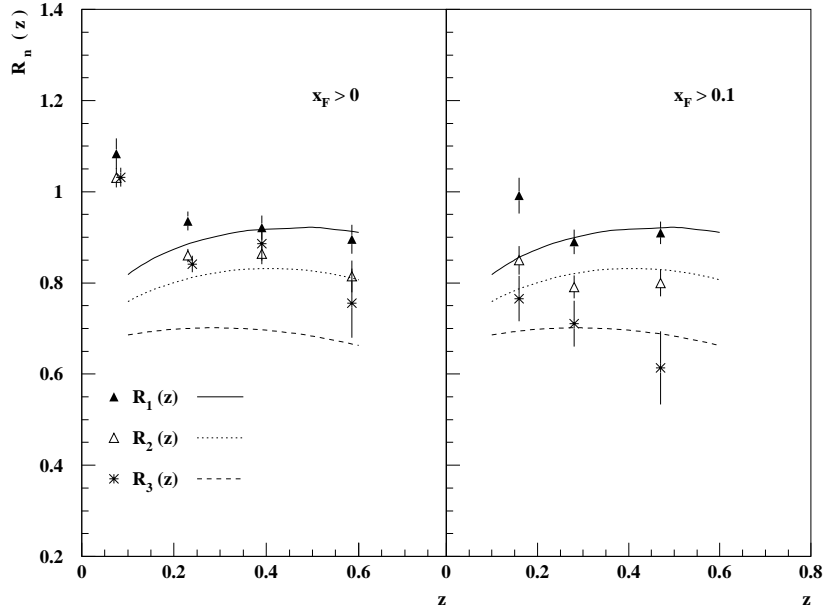


Figure 3: The dependence of $R_n(z)$ on the z variable of the "trigger" hadron at $x_F > 0$ (the left panel) and $x_F > 0.1$ (the right panel) The curves are the TSM predictions (see text).

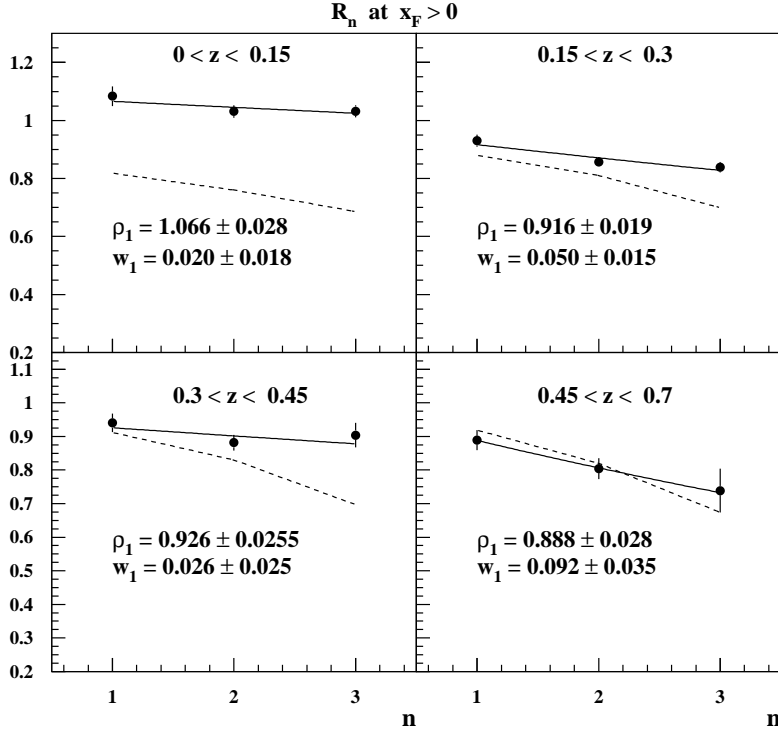


Figure 4: The n -dependence of $R_n(z)$ for different z -ranges of the "trigger" hadron at $x_F > 0$. The solid lines are the fit results, while the dashed lines are the TSM predictions (see the text).

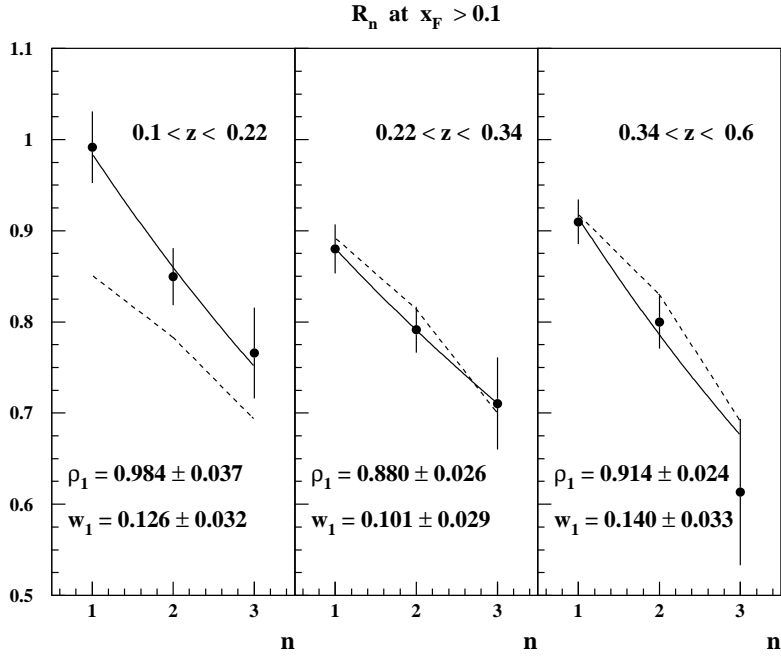


Figure 5: The same as Fig. 4, but at $x_F > 0.1$.

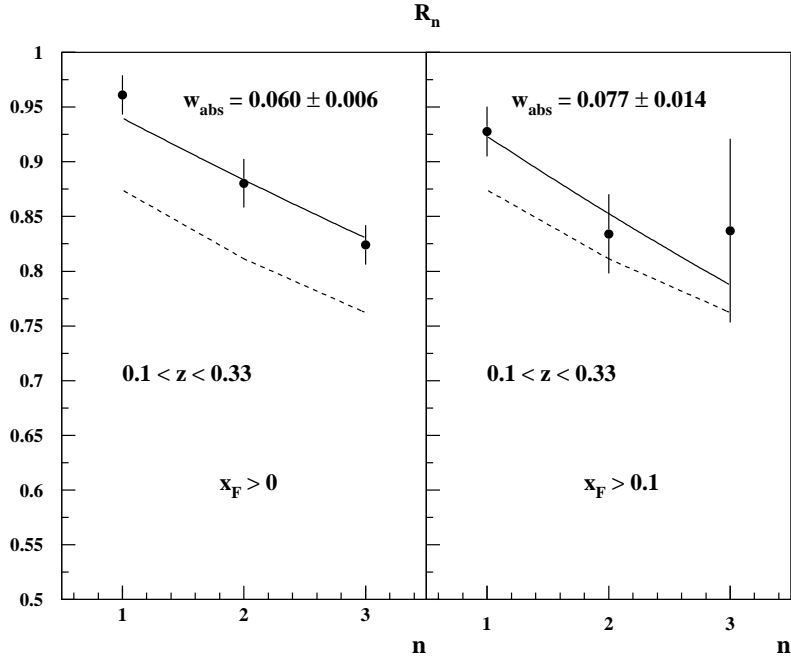


Figure 6: The dependence of $R_n(z)$ on the number n of involved hadrons with $0.1 < z < 0.33$ and $x_F > 0$ (the left panel) and $x_F > 0.1$ (the right panel). The solid lines are the fit results, while the dashed lines are the TSM predictions (see the text).